ENGINEERING RESEARCH JOURNAL (ERJ)

Vol. 1, No. 47 Jan. 2021, pp 66- 74

Journal Homepage: http://erj.bu.edu.eg

Combustion Modeling for Turbulent Premixed Propane-Air Mixture

Mohamed M. S. Yaseen[a], R.Y. Sakr[b], R.I. Afify[b], M. W. El-Dosouky[b]

[a] Graduate Student ,[b] Mechanical Engineering Dept., Faculty of Engineering at Shoubra, Benha University

Abstract: In the present study, ANSYS Fluent Computational Fluid Dynamics CFD package is utilized to analyze the combustion of premixed propane/air mixture in a cylindrical combustion chamber surrounded by an annular space where cold water enters to and exits from the annular space, simply simulating gas/water heater. The combustion process is assumed to take place in one step (one reaction). Species transport and finite rate/eddy dissipation is used. The flow is assumed to turbulent and standard k-ε is employed.

The effect of the equivalence ratio, ϕ, (0.55-1.0) and the inlet gas mixture temperature (400K-600K) on the combustion process in investigated. The temperature and species mass fractions as well as their contours are presented. Also, the combustion efficiency and the heat release rate

1. INTRODUCTION

The increasing cost of experimental tests and the efforts to reduce the development time for modern combustor design. The efficient design of modern combustors needs the development of more efficient, reliable and robust numerical models. Turbulent combustion model with detailed chemical kinetics is needed for accurate predictions of flame stability and pollutant emissions. Reynolds-average Navier-Stokes RANS based combustion models have been the backbone in industrial CFD applications and have been studied by many investigators for the last few decades [1, 2, 3]. The RANS require relatively modest computing resource and time because they solve the averaged quantities and models the small scale fluctuating quantities. Maele et al. [2] utilized and compared the RANS based turbulence models, namely standard k-ε, realizable k-ε and RNG k-ε turbulence models to the swirling flames in the Sydney burner. It was noticed that the realizable k-ε model yielded slightly better flow field. Dally et al [1] modified the value of a constant in the dissipation transport equation of the standard k-ε model and found that the modified k-ε gives better results than the Reynolds stress model RMS for bluff body flame. The comparison between the standard k-ε model, the modified k-ε model and the RMS model is carried out by frassoldati et al. [3] and they found that the modified k-ε gives better predictions for fuel jet dynamics than RSM.

Fiorina et al. [4] combined both the tabulated chemistry obtained from premixed flamelets and presumed probability density function (PDF) approaches to carry out RANS modeling of premixed turbulent combustion. They investigated a high velocity fluctuations flame with a thickened-wrinkled structure and proposed a scalar dissipation rate that implies an assessment of the coupling between micromixing and flame wrinkling Bray et al. [5] applied the reduced chemical kinetic mechanisms in turbulent premixed flames models, at high Damköhler numbers for hydrogen–air and methane–air systems. They used the (PDF) of two independent scalar variables. Richardson et al. [6] analyzed the mixing time scale in direct numerical simulations (DNS) of 3-D, with reduced CH_4–air chemistry in the thin reaction zones regime of turbulent Bunsen flames. They showed that the mixing rates are affected by the high gradients which are attained by the structures of flamelet at high Damköhler numbers. The reduction techniques for chemical kinetics emphasizing on combustion process are reviewed comprehensively in [7-11].

Tang et al. [12] developed a 3-D CFD model using an embedded skeletal reaction mechanism for premixed H_2-air combustion in the micro combustor for thermo-photovoltaic system. The radiation wall of the new combustor design

indicated a higher mean temperature due to the augmentation of heat transfer, and this was more significant at higher plate number. One of the efficient techniques to model the flame front in turbulent premixed combustion is the thickened flame TF model. To simulate the pollutant formation, ignition and extinction, the multistep reaction mechanisms become more important. Gau et al. [13] found incomplete combustion in either laminar or turbulent conditions for the coupling of TF model with multistep reaction mechanisms and proposed that the modified dynamic thickened flame sensor is suitable for multistep reaction.

Propane is a clean fuel and one of the constituents of natural gas which can be liquefied at high pressures and easy transported. It is used as fuel for jet engines in the form of liquefied petroleum gas LPG for car engines. The present work investigated the effect of operating conditions such as ϕ and inlet gas mixture on the turbulent premixed combustion of water/gas heater.

2- SPECIES TRANSPORT THEORY AND FINITE RATE CHEMISTRY

The mixing and transport of chemical species can be modeled using Fluent-Ansys by solving the conservation equations that describes convection, diffusion and reaction for each element species. Simultaneous chemical reaction can be modeled here as a volumetric reaction.

2.1 Species transport equations

The mass fraction of each species, Y_i can be obtained by solving the conservation equation for the i^{th} species that can be written as:

$$\frac{\partial}{\partial t}(\rho Y_i) + \nabla.(\rho \vec{v} Y_i) = -\nabla \vec{J}_i + R_i + S_i \quad (1)$$

Where;

R_i = the net production rate of species i by chemical reaction and

S_i = the rate of creation by addition from the dispersed phase and any other sources.

2.2 Mass diffusion in laminar flows

In laminar flows, the diffusion flux $\vec{J}i$ of species i in Eq. (1), which results from concentration and temperature gradients can be expressed as:

$$\vec{J}_i = -\rho D_{t,m} \nabla Y_i - D_{T,j} \frac{\nabla T}{T} \quad (2)$$

Where;

$D_{i,m}$, $D_{T,i}$ are the mass and the thermal (Soret) diffusion coefficients respectively

2.3 Mass diffusion in turbulent flows

The mass diffusion in turbulent flow takes the form:

$$\vec{J}_i = -(\rho D_{t,m} + \frac{\mu_t}{Sc_t}) \nabla Y_i - D_{T,i} \frac{\nabla T}{T} \quad (3)$$

Where

Sc_t = the turbulent Schmidt number ($Sc_t = \mu_t / \rho D_t$)

μ_t = the turbulent viscosity.

D_t = the turbulent diffusivity.

In many multicomponent mixing flows, the transport enthalpy due to diffusion of species is given by: $\nabla.\left[\sum_{i=1}^{n} h_i \vec{J}_i\right]$ which affect significantly when Lewis number is far from unity.

$$Le_i = \frac{K}{\rho C_p D_{i,m}}$$

The reaction rate that appear as a source term in Eq. (1) is computed in Fluent-Ansys by one of the three models, the first is laminar finite rate model, the second is the eddy dissipation model and the third one is eddy dissipation concept. Detailed descriptions of these models are given in [14].

3. PROBLEM DEFINITION

3.1 Computational Domain and grid

The current work investigates the combustion of propane in cylindrical combustion chamber surrounded by a cylindrical annulus in which filled with cold water to be heated and exit from the annulus. The schematic diagram of the physical model is presented in Fig. (1).

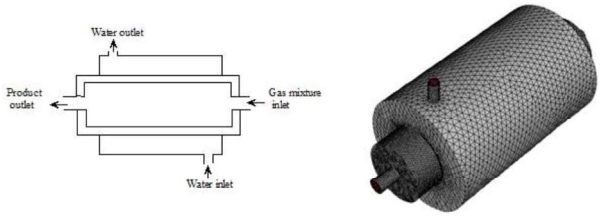

Fig. 1 schematic diagram and comuptational grid

3.2 Mathematical Modeling

3.2.1 Turbulence Model

The standard two-equation, k-ε turbulence model with standard values was used for this study. The k-ε turbulence model consists of the turbulent kinetic energy and dissipation equations given below:

$$\frac{\partial k}{\partial t} + \nabla.(\rho \vec{u} k) = \nabla.\left\{\left[\mu_{lam} + \frac{\rho \nu_t}{\sigma_k}\right] \nabla k\right\} + \rho \nu_t G - \rho \varepsilon \quad (4)$$

$$\frac{\partial \varepsilon}{\partial t} + \nabla.(\rho \vec{u} \varepsilon) = \nabla.\left\{\left[\mu_{lam} + \frac{\rho \nu_t}{\sigma_\varepsilon}\right] \nabla \varepsilon\right\} + C_{1\varepsilon} \rho \nu_t G \frac{\varepsilon^2}{k} - C_{2\varepsilon} \rho \frac{\varepsilon^2}{k} \quad (5)$$

where G represents the turbulent generation rate which is equal to

$$G = 2\left\{\left[\frac{\partial u}{\partial x}\right]^2 + \left[\frac{\partial v}{\partial y}\right]^2 + \left[\frac{\partial w}{\partial z}\right]^2\right\} + \left(\frac{\partial u}{\partial y} + \frac{\partial v}{\partial x}\right)^2 + \left(\frac{\partial u}{\partial z} + \frac{\partial w}{\partial x}\right)^2 + \left(\frac{\partial w}{\partial y} + \frac{\partial v}{\partial z}\right)^2 \quad (6)$$

In the execution of this model the Kolmogorov-Prandtl expression for the kinematic turbulent viscosity, ν_t is used and it is given by:

$$\nu_t = C_\mu \frac{\varepsilon^2}{k} \quad (7)$$

In the equations above Cμ, σk, σϵ, C1μ, and C2μ are all taken to be constants and are given their usual standard values of: 0.09, 1.0, 1.3, 1.44 and 1.92 respectively.

3.2.2 The Species Model

The species were modeled using the model based on the work published by Westbrook and Dryer (1981). This simplified model consists of one chemical reaction and 5 species.

3.2.3 Turbulent Gaseous Combustion Model

The turbulence-chemistry interaction (gaseous combustion) was modeled using the finite-rate/eddy dissipation model. Essentially, the net rate of reaction is the minimum of the following:

- The chemical production or depletion term (kinetic rate)
- The rate of dissipation of reactant eddies
- The rate of dissipation of product eddies

3.2.4 Boundary Conditions

Air/fuel mixture Inlet:
Inlet velocity = 3 m/s
Turbulence intensity = 3.6 %
Turbulence length scale = 0.003 m

Inlet temperature was varied to take the values of 400K, 500K, and 600K respectively.

Also, species mass fraction was determined according to the studied equivalence ratio.

Combustion gases outlet:
Outlet gauge pressure =0
Backflow temperature = 1000K
Outlet species mass fractions depend on the equivalence ratio.

Water inlet
Inlet velocity = 0.25 m/s
Inlet temperature = 298 K

Water outlet:
Outlet gauge pressure =0

Wall boundary conditions:
No slip condition
Adiabatic boundary condition.

3.3 Method of Solution

3.3.1 Stability and convergence

It is difficult to obtain a convergent solution for reacting flow because of the strong impact of the chemical reaction on the basic flow pattern and the strong coupling between mass and momentum equations and species transport equations. Also, the large heat release from the reaction causes high density change and a large acceleration in the flow. Theses coupling issues are solved by using two steps solution technique. When the reaction rate kinetics is more rapid than the rate of convection and diffusion the solution of species transport becomes more difficult and such system is terms as “stiff” and the coupled solver is recommended for laminar flow and eddy dissipation concept is recommended for turbulent flow.

3.3.2 Two-step procedure

To reach a stable converged solution in a reacting flow two-step process can be a practical solution. This can be achieved by solving the governing equations with disabling the reaction i.e. (cold/non-reacting) flow. After reaching the basic flow pattern the reaction can be enabled.

3.3.3 Ignition in combustion simulation

Practically, to initiate the spontaneous ignition for fuel/air mixture, the temperature of the mixture should exceed the activation energy threshold requirements. The same issue is made in the current simulation. Finite rate eddy dissipation model for chemistry-turbulence interaction is used. The initial spark was supplied by patching a high temperature field (1000K) into the computational domain of combustion. It is being noted that the initial patch has no effect on the final steady state solution.

3.3.4 The solver

The gradient least square cell based method was applied for spatial discretization schemes and second order upwind scheme was employed for density, momentum, modified turbulent viscosity and energy equations. Under relaxation factor of 0.8 was used for species, energy and density while a value of 0.6 was applied for momentum, turbulent kinetic energy, turbulent kinetic dissipation rate and turbulent viscocity.

4. RESULTS AND DISCUSSIONS

4.1 Model Validation

To check the reliability of the present model, its predictions were compared with that of previous work of Anetor et al. [15], for premixed propane-air oxidation in a conical reactor for five chemical reactions and twelve species. Reasonable

agreement is observed in Fig. (2), the slight differences between the results may be due to the difference in geometry dimensions.

4.2 Effect of Equivalence Ratio

The effect of equivalence ratio in the range of study from lean to chemically correct gas mixture on the combustion process is illustrated in Fig. (3). The temperature distribution along the centreline of the combustion chamber for different equivalence ratio with inlet fuel/air mixture of 500 K and inlet fuel/air mixture of 3 m/s is demonstrated in Fig. (3a). It is noticed from the figure that the temperature is kept constant till the reaction zone reaching its maximum value then it decreases. Also, as the equivalence ratio increases the temperature of reaction products increases and this is due to the decrease of the excess air in the fuel/air mixture. Also, the effect of the equivalence ratio on the variation of C_3H_8 species distribution along the combustion chamber centreline is depicted in Fig. (3b). The fuel species starts from the inlet boundary value and kept constant for some distance till the reaction starts then it decreases reaching zero value at the which the reaction stops. Also, the variation of CO_2 species distribution is depicted in Fig. (3c). the figure shows that the distribution of CO_2 is in contrast of C_3H_8 species distribution and this is logic one element of reactants against one element of product. Insignificant dependence on ϕ for starts and ends is observed (the reaction zone length). Also, it is noticed that the starts and ends locations are the same for both distributions while there is lag and advance between species distributions compared with temperature distribution and this may be due to the heat capacity of the system.

The temperature contours and mass fraction contours of species C_3H_8, CO_2, H_2O for equivalence ratio of 0.6 and 0.8 for inlet velocity of 3 m/s and inlet temperature of 500 K are illustrated in Fig. (4). It is noted from the figure, that the maximum temperature increases with the increase of the equivalence ratio and the flame triangle becomes thinner. Also, the maximum mass fraction of C_3H_8, CO_2, and H_2O species increases with the increase of the equivalence ratio.

4.3 Effect of Equivalence Ratio

The inlet effect of Propane/air mixture temperature on the combustion process is given in Fig. (5). The temperature distribution along the centreline of combustion chamber is illustrated in Fig. (5a). It is shown from the figure that as the inlet temperature increases, the combustion process starts nearer to the mixture inlet and higher product temperature is attained. The effect of inlet temperature on the C_3H_8 mass fraction distribution is depicted in Fig. (4b) and CO_2 distribution in Fig. (5c). Also, it is observed that the starts and ends of species changes from maximum to minimum for C_3H_8 and from minimum to maximum for CO_2 are the same for inlet fuel/air mixture temperatures.

The temperature contours and mass fraction contours of species C_3H_8, CO_2, H_2O for inlet temperature of 400 K and 600 K for equivalence ratio of 0.7 and inlet velocity of 3 m/s are demonstrated in Fig. (6). It is noticed from the figure, that the maximum temperature increases with the increase of the inlet temperature and the reaction zone becomes smaller. Also, this is confirmed from the mass fraction of C_3H_8, CO_2, and H_2O species contours.

4.5 Combustion Performance Parameters

4.5.1 Combustion Efficiency

The combustion efficiency is calculated as follows:

The heat liberated from the combustion process is directed to heat the both the water and Propane/air mixture.

$$Q_w = m_w \cdot cp_w (T_{wo}-T_{wi}) \quad (8)$$

$$Q_g = m_g\, cp_g (T_{go}-T_{gi}) \quad (9)$$

$$Q_f = Q_w + Q_g \quad (10)$$

So, the efficiency of the combustion process (water gas heater) can be expressed as:

$$\eta = Q_w/Q_f \quad (11)$$

Figure (7) shows the variation of the combustion efficiency with the equivalence ratio for different inlet mixture temperature. It is observed from the figure that as the equivalence ratio increases the combustion efficiency decreases and as the inlet temperature increases the combustion efficiency increases.

4.5.1 Heat Release Rate

The heat release rate HRR is calculated from:

$$HHR = Q_f/V_c \quad (12)$$

Where, V_c is the coolant volume, and given by:

$$Vc = \pi/4\,(D_o^2 - D_i^2)\,L, \quad (13)$$

The variation of HRR with the equivalence ratio for different inlet mixture temperature is shown in Fig. (8). it is depicted from the figure that as the equivalence ratio increases the HRR increases and the HRR increases with the decrease of inlet mixture temperature.

5 CONCLUSIONS

From the findings of the current work, the temperature of reaction products increases and the flame triangle thinner with the increase of ϕ and insignificant dependence of the reaction zone length on ϕ. As the inlet temperature increases the temperature of the reaction products increases and shorter reaction zone. The increase of ϕ leads to the combustion efficiency decrease and as the inlet temperature increases the combustion efficiency increases. The increase of ϕ results in HRR increase and the HRR increases with the decrease of inlet mixture temperature increases the HRR increases and the HRR increases with the decrease of inlet mixture temperature

REFERENCES

[1] Dally, B. B., Feltcher, D. F., and Masri, A. R., 1998, "Flow and mixing fields of turbulent bluff-body jets and flames," Combustion Theory and Modelling, 2(2), pp. 193-219.

[2] Maele, K. V., Merci, B., and Dick, E., 2003, "Comparative study of k-ε turbulence models in inert and reacting swirling flows," 33rd AIAA Fluid Dynamics Conference and Exhibit, 2003-3744.

[3] Frassoldati, A., Sharma, P., Cuoci, A., Faravelli, T., and E., R., , "Kinetic and fluid dynamics modeling of methane/hydrogen jet flames in diluted coflow," Applied Thermal Engineering, 30(4), (2010), pp. 376-383.

[4] Fiorinaa, B., Gicquela, O., Vervischc, L., Carpentier, S., and Darabiha, N., " Premixed turbulent combustion modeling using tabulated detailed chemistry and PDF", Proceedings of the Combustion Institute 30 (2005), pp. 867–874.

[5] Bray, K., Champion, M., and Libby P.A., "Systematically reduced rate mechanisms and presumed PDF models for premixed turbulent combustion", Combustion and Flame 157 (2010), pp.455–464.

[6] Richardson, E.S, Grout, R.W., Sankaran, R., and Chen, J.H., "Numerical analysis of reaction–diffusion effects on species mixing rates in turbulent premixed methane–air combustion", Combustion and Flame 157 (2010), pp. 506–515.

[7] Herbinet, O., Pitz, W.J. and Westbrook, C.K. "Detailed chemical kinetic mechanism for the oxidation of biodiesel fuels blend surrogate," Combustion and Flame, vol. 157, (2010), pp. 893-908.

[8] Shi, Y. Ge, H. W., Brakora, J. L., and Reitz, R. D., "Automatic chemistry mechanism reduction of hydrocarbon fuels for HCCI engines based on DRGEP and PCA methods with error control," Energy and Fuels, vol. 24, (2010), pp. 1646-1654.

[9] Lu T. and Law C. K., "A directed relation graph method for mechanism reduction," Proceedings of the Combustion Institute 30(1): (2005), pp. 1333-1341.

[10] Hautman, D.J. Dryer, F.L. Schug, K.P. and Glassman, I. "Multiple-step overall kinetic mechanism for the oxidation of hydrocarbons," Combustion science and technology, vol. 25, (1981), pp. 219-235.

[11] Kagwanpongpan, T. and Krautz, H. J. "Numerical simulation of lignite combustion in O2–CO2 environment by eddy-dissipation model," in 1st International Oxyfuel Combustion Conference 2009, Radisson SAS Hotel, Cottbus, Germany, 7-11 Sept. 2009.

[12] Tang, A., Pan, J., Yang, W., Xu, Y. and Hou, Z., "Numerical study of premixed hydrogen/air combustion in a micro planar combustor with parallel separating plates", international journal of hydrogen energy 4 0 (2 0 1 5), 2396-2403.

[13] Guo, S., Wang, J., Wei, X., Yu, S., Zhang, M. and Huang, Z., "Numerical simulation of premixed combustion using the modified dynamic thickened flame model coupled with multi-step reaction mechanism", Fuel 233 (2018) 346–353.

[14] ANSYS Fluent User's Guide. Release 15.0, ANSYS, Inc. November 2013.

[15] Anetor, L., Osakue, E., Odetunde, C., "Reduced Mechanism Approach of Modeling Premixed Propane-Air Mixture Using ANSYS Fluent", Engineering Journal, Volume 16 Issue 1.

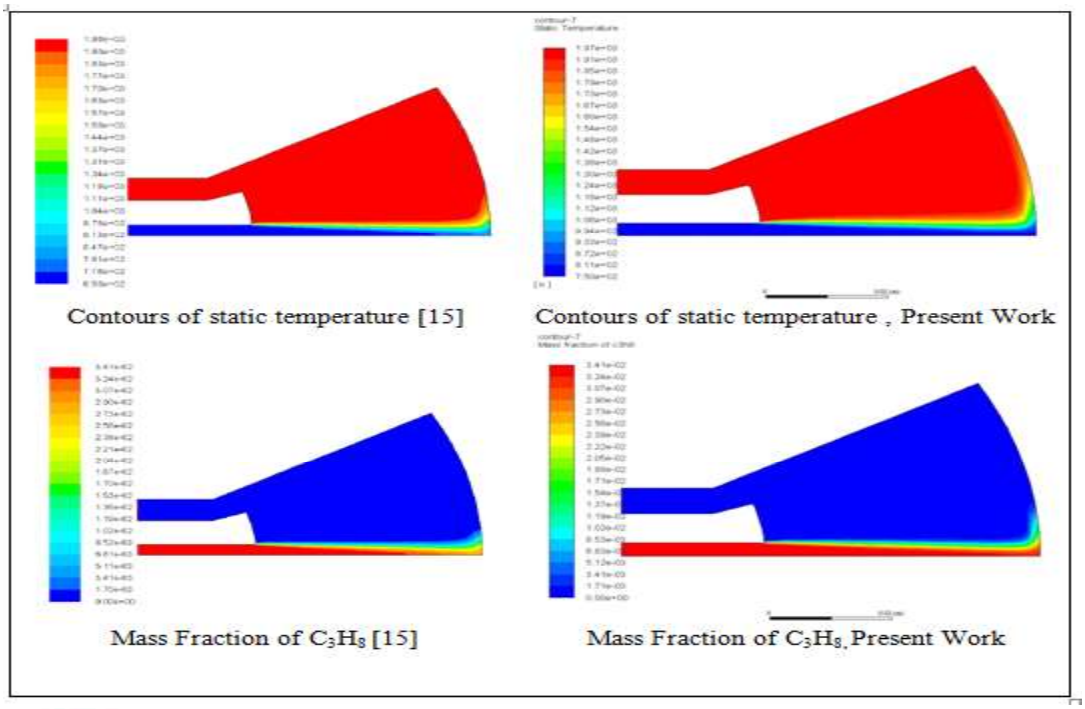

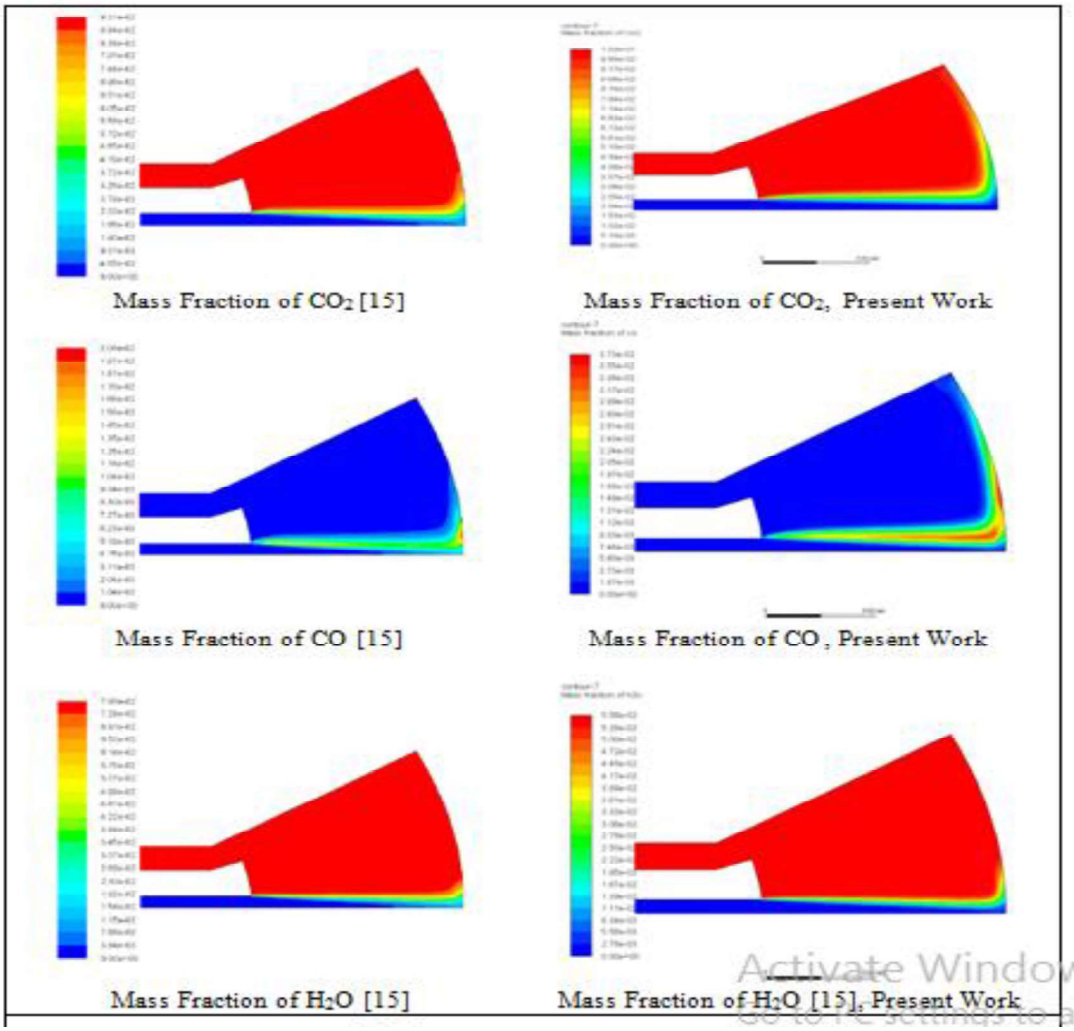

Fig. (2) Comparison between the present model predictions and results in [15]

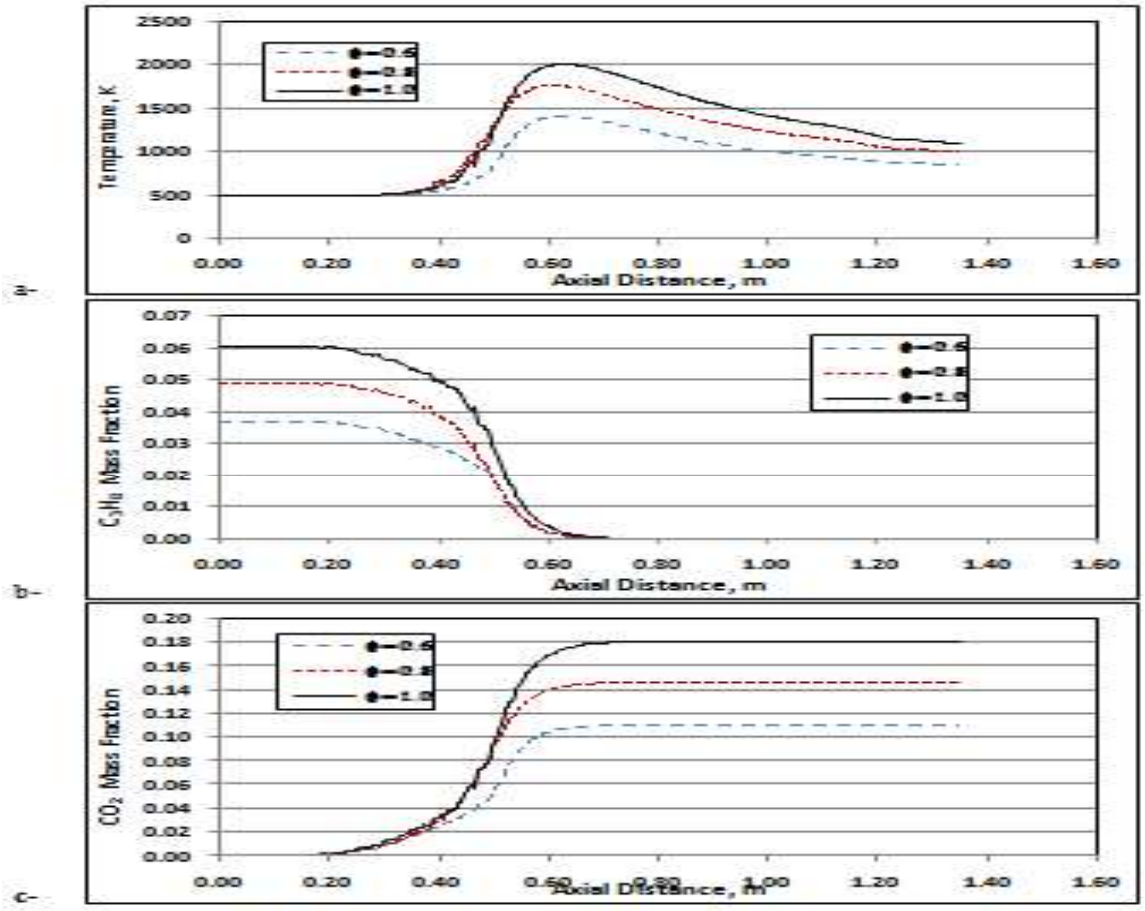

Fig. (3) Effect of Equivalence Ratio on Temperature, C_3H_8 and CO_2 Mass Fraction Distributions at Combustor Centreline for Tin= 500 K

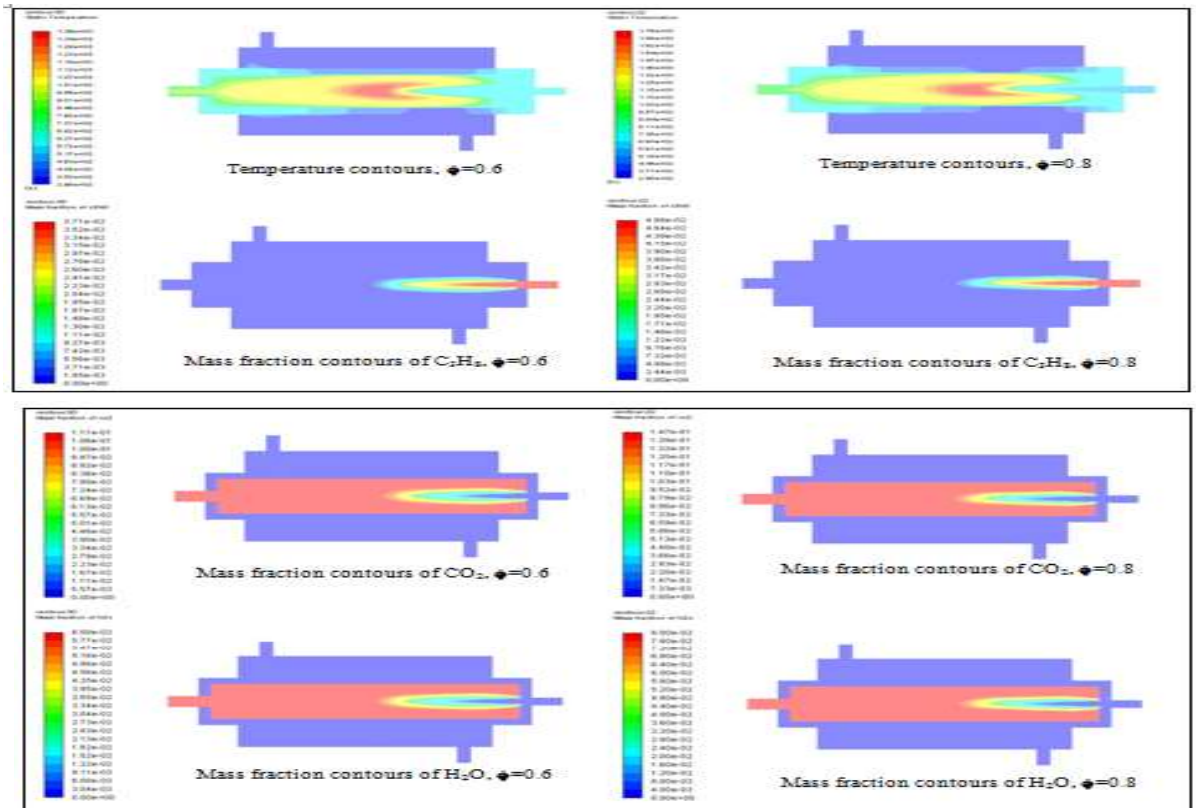

Fig. (4): Coutours for the temperature and some species for equivalence ratio of o.6 and 0.8 at V_{in} = 3 m/s and T_{in}= 500 K

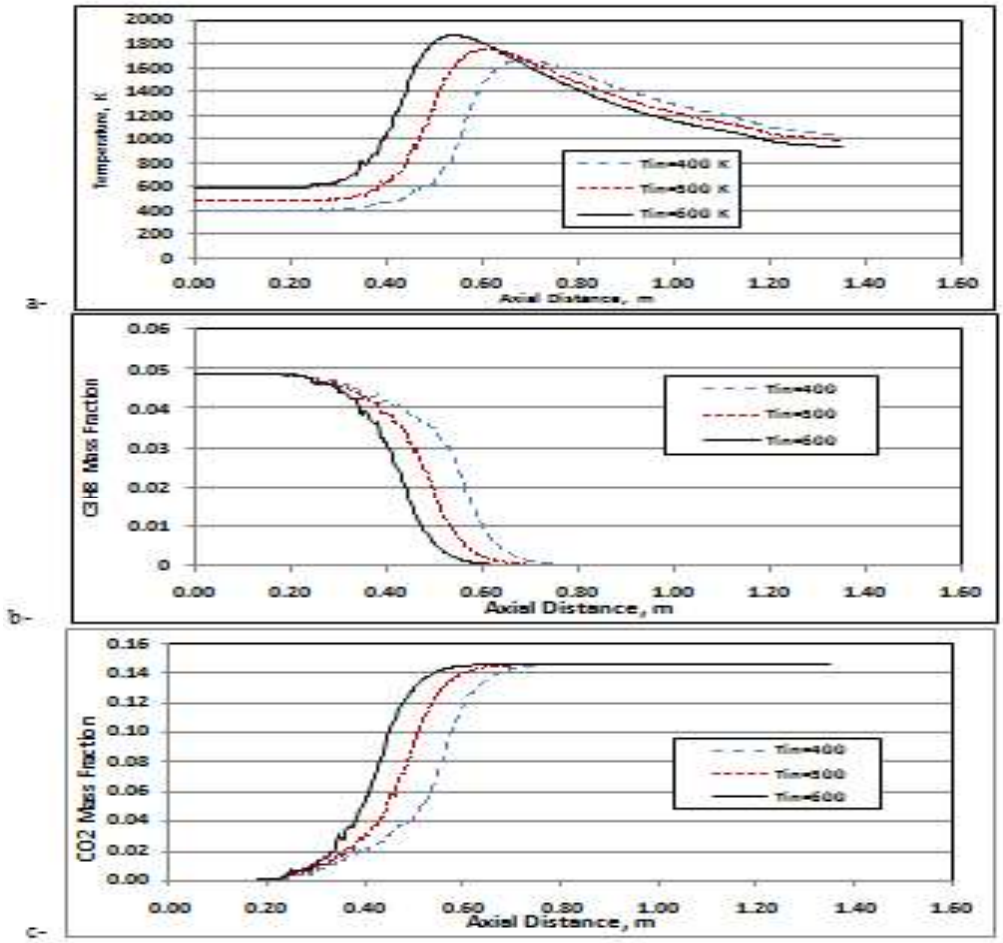

Fig. (5) Effect of Inlet Mixture on Temperature, C_3H_8 and CO_2 Mass Fraction Distributions at Combustor Centreline for $\phi = 0.8$

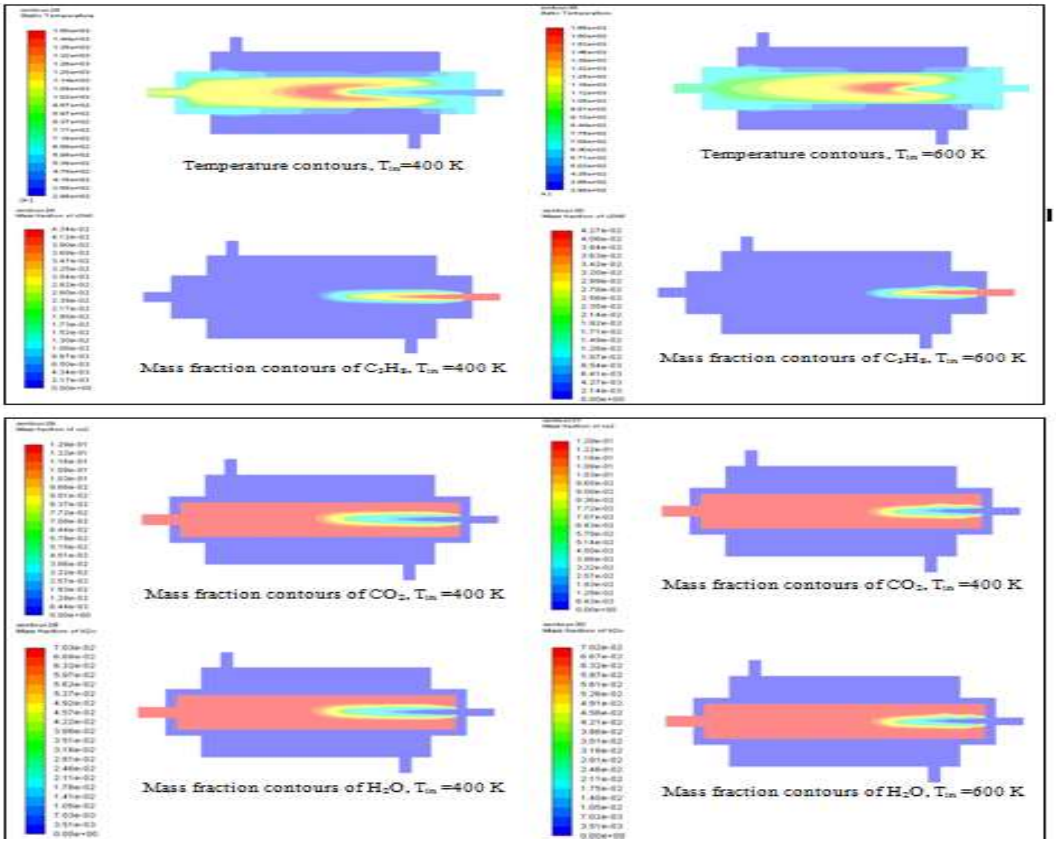

Fig. (6): Coutours for the temperature and some species for inlet Temperasture 400 K, 600 K at V_{in} = 3 m/s and ϕ= 0.7

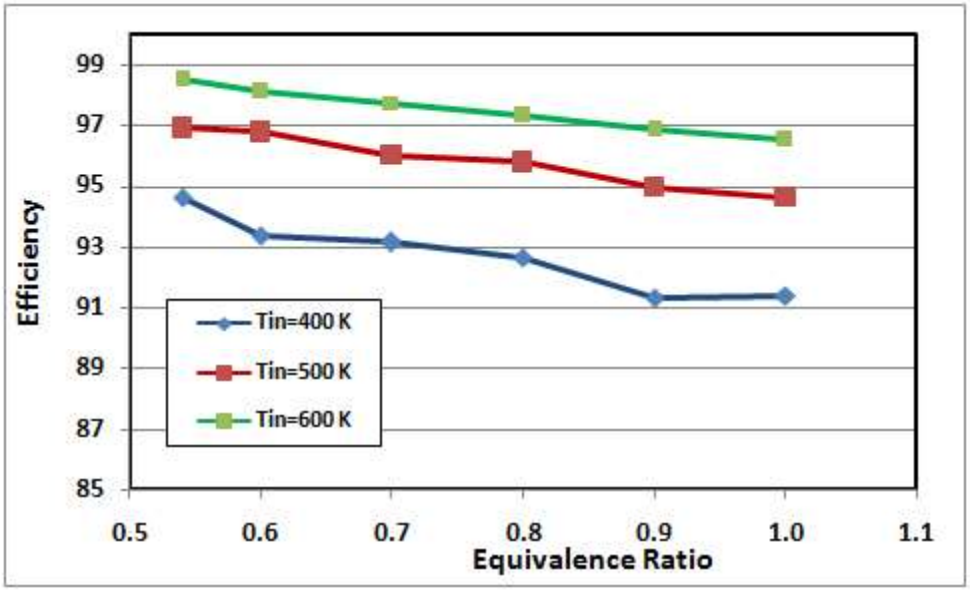

Fig. (7): Variation of combustion efficiency in the water heater with the equivalence ratio for different inlet mixture efficiency, Vin =3 m/s

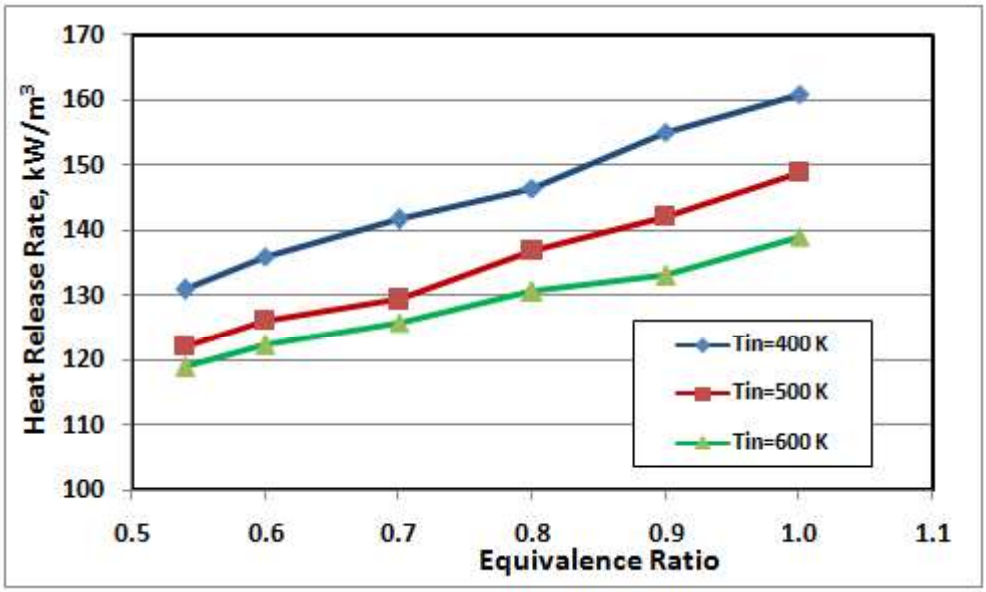

Fig. (8): Variation of heat release rate in the water heater with the equivalence ratio for different inlet mixture efficiency, Vin =3 m/s